Phys-ga2000: Point Spread Function of a Telescope

Marco Borja, Adam Guerin, and Ben Johnston
(Dated: December 15, 2023)

When light enters a telescope, in the ideal on-axis case, it will all be focused to a single point. But, due to the wave properties of light, instead of going to a point it will form a finite image at the focus. How and where the light will be focused depends on what is known as the point spread function of the telescope. The point spread function modulates the image that a telescope is able to deliver to an observer, and it depends on different properties of the telescope such as the shape of and imperfections in the telescope. By convoluting the point spread function with an example incoming light source we can produce an example image that would be produced by the telescope. In this paper we go over how to calculate and different use cases for the point spread function in different situations.

I. INTRODUCTION

The point spread function can be shown to be the squared amplitude of the complex pupil function [1]:

$$P(x,y) = P_r(x,y)e^{\frac{-i2\pi W(x,y)}{\lambda}} \tag{1}$$

where $P_r \in \{0,1\}$ is a function of position on the aperture, W is a phase shift and λ is the wavelength of the light wave. If we consider the focal plane coordinate system of x_f and y_f the PSF can be written as [1]:

$$PSF(x_f,y_f) = FT[P(x,y)]\left(k_x = \frac{x_f}{\lambda f}, k_y = \frac{y_f}{\lambda f}\right) \tag{2}$$

where f is the focal length and k_x is the Fourier transform evaluated at $\frac{\theta_x}{\lambda}$, and the same in y. We call it θ as it corresponds to the incoming angle on the sky.

In the simplest case, $P(r,\theta)$ is 1 within a radius $\frac{D}{2}$ and 0 outside - in this situation the image formed is known as the Airy pattern and is given by [2]:

$$I = C\left(2\frac{J_1(\pi r D/\lambda f)}{\pi r D/\lambda f}\right)^2 \tag{3}$$

where J_1 is the first-order Bessel function. The characteristic size of the Airy pattern is given by [3]:

$$\frac{2.44\lambda f}{D} \tag{4}$$

A. Prep work

The first-order Bessel function can be calculated using the following formula [4]:

$$J_1 = \frac{1}{\pi}\int_0^\pi d\theta \cos(\theta - x\sin\theta) \tag{5}$$

In general this integral could have been done using numerical libraries available through Python, however NumPy uses very accurate analytic approximations to evaluate functions as opposed to using explicit integrals. Therefore for the purposes of this study Simpson's rule was used to check NumPy's implementation of the calculation. This code was used repeatedly throughout this study for the purpose of calculating the point spread function, as will be seen in the following sections.

Many reflective telescopes have a Cassegrain design, which consists of a primary concave mirror and a secondary convex mirror, resulting in an aperture in the shape of a donut with a hole in the middle (as seen below in *Figure 1*) [5]. The main purpose of this kind of design is that the arrangement of mirrors fold the optical path onto itself relative to the primary aperture, which produces a very large focal length [6]; this makes such designs suitable for planetary observations or other high-resolution imaging.

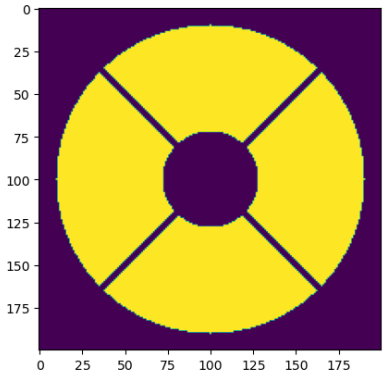

FIG. 1: Cassegrain aperture.

Note here that the diagonal lines in the above figure come from the fact that in order to hold the secondary mirror in place there are structural elements in the form of several struts which cause obstructions within the aperture (small lines with $P = 0$ aligned radially) [1].

It is possible to write the point spread function for the

Cassegrain telescope design in terms of the first-order Bessel function as seen below [7]:

$$I(r) = \frac{I_0}{(1-\epsilon^2)^2}\left(\frac{2J_1(\frac{\pi r D}{\lambda f})}{\pi r D/\lambda f} - \frac{2\epsilon J_1(\frac{\epsilon \pi r D}{\lambda f})}{\pi r D/\lambda f}\right)^2 \tag{6}$$

where I_0 is the maximum intensity and $\epsilon \in \{0, 1\}$ is the ratio of the secondary mirror to the diameter of the aperture itself. This point spread function for both Eq (3) and (5) has been plotted and can be seen below in *Figure 2*:

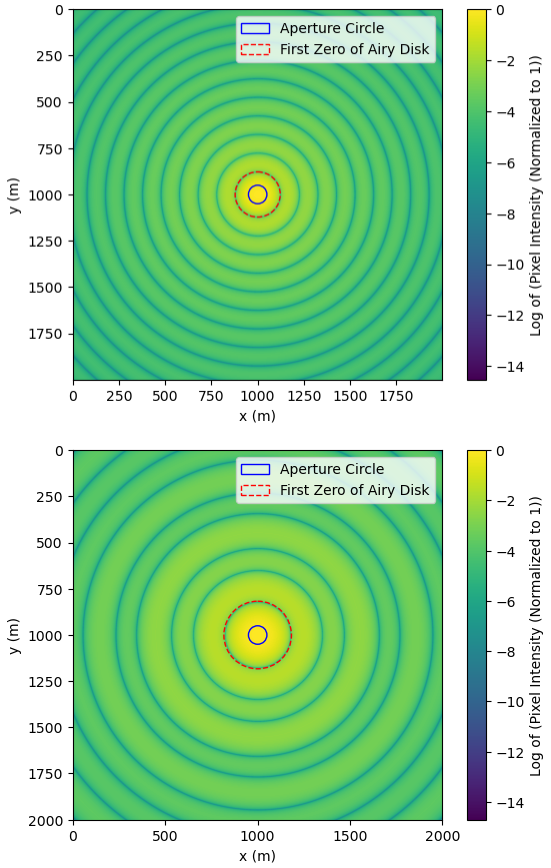

FIG. 2: Top: PSF for circular aperture . Bottom: PSF for Cassegrain aperture.

These two PSFs are very similar, both have circular symmetry with repeating zeros, but the Cassegrain ends up with wider spacing between the zeros because the zeros only appear when either both the open aperture, and the block are zero, or when they are equal in magnitude. This ends up with a different length scale that leads to a potentially more desirable image.

One aim of this study is to simulate imperfections in the phase of the incoming light rays that arise via different sources. Therefore Gaussian random fields were generated using NumPy's random.normal and fast Fourier transform functions. Gaussian random fields are extremely well known and have many different applications due to the fact that they are convenient mathematical objects completely defined by their mean and covariance functions [8]. They are an example of a statistical description of a system that require very simple assumptions to understand the properties of many structures encountered in nature and can be generated by choosing random independent values from Gaussian distributions for Fourier modes in $\vec{k}$-space before converting back to configuration space via an inverse Fourier transform. Only two parameters are needed to produce such fields, namely a zero mean and a variance that is a function known as the power spectrum, $P(k)$ [1, 9]. Such spectra describe clustering in terms of wavenumber k that separates the effects of different scales [10]. The formula used for the power spectrum in this study is given by [1]:

$$P(k) \propto k^n \exp\left(-\frac{k^2}{k_c^2}\right) \tag{7}$$

First, a function was written that returns a set of amplitudes $a(\vec{k})$ for each mode and subsequently this, along with values for $a(\vec{k})$ were used to produce such random fields with $P(k)$ for several values of $n < 0$ and k_c as seen in *Figure 3*:

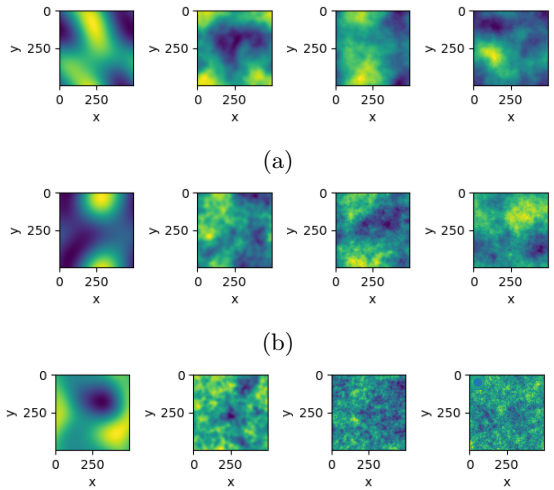

FIG. 3: From left to right on all images increases the values of k_c. (a) $n = -4$. (b) $n = -3$. (c) $n = -2$

The power spectrum tells you the relevance of specific length scales, therefore for a larger associated power with smaller wave numbers k you expect larger length scales to dominate. Similarly for a larger associated power with larger wave numbers you expect smaller length scales to dominate as the wave number goes as $\frac{1}{L}$, L being length. In this case k_c controls an exponential cut off, and as a result for small k_c larger wave numbers quickly die away, but if k_c is larger then larger wave numbers can stay relevant for longer until $k > k_c$. The power law scaling in $P(k)$ tells you how much to weigh the specific powers

that haven't been cut off by the exponential decay. This is why the k^{-4} random fields look similar, any higher order terms that did survive are still overpowered by small wave numbers (long wavelengths). As the power law decreases in potency the smaller wavelengths become relevant again, which is why the random fields get smaller structures as you move to the right (k_c getting larger). When $k_c = 100$ and $n = -2$ is reached, we arrive at something that looks similar to what most people would call white noise.

II. CALCULATING IDEAL PSFS

In order to verify the result seen previously in *Figure 1*, a numerical fast Fourier transform (FFT) was performed on a simple circular aperture and the point spread function was computed. To make sure that the aperture was simulated in isolation, the size of the computational grid was at least twice the size of the aperture itself. The results of this calculation can be seen in *Figure 4* for various choices of the grid resolution and size relative to the aperture, along with the residuals between the numeric and analytic calculations.

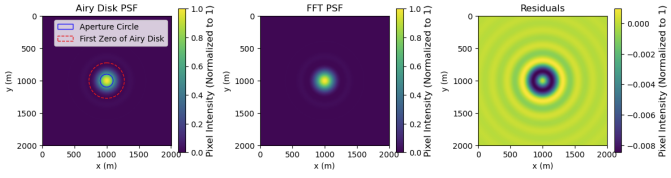

FIG. 4: Comparison of PSF of a circular aperture calculated using the analytical airy disk solution, and the fast Fourier transform solution. Residuals are then calculated and presented in the third graph. Both PSF graphs were calculated using resolution = 2001, wavelength = 150, focal length = 300, and aperture diameter = 200.1

Most of the image will be focused to the center, so that is where we would expect most of the error to be concentrated. By choosing a large enough resolution and a small enough aperture we can avoid most of the unphysical boundary effects. If we had done larger resolution it would've been more accurate, but at this level, of only doing a 2000 by 2000 grid and an aperture a tength the size of the grid, the max error is still below 1 percent at any point.

Further analysis was then undertaken in order to investigate how the point spread function varies with aperture size, the results of which are presented in *Figure 5*.

A good way of understanding this change in PSF with changing aperture size is with cameras. Wider apertures gives a narrower depth of field, you focus in more on a single point. With a narrower aperture you get a wider depth of field, in a more extreme case, one could think about a pinhole camera or camera obscura, where a very

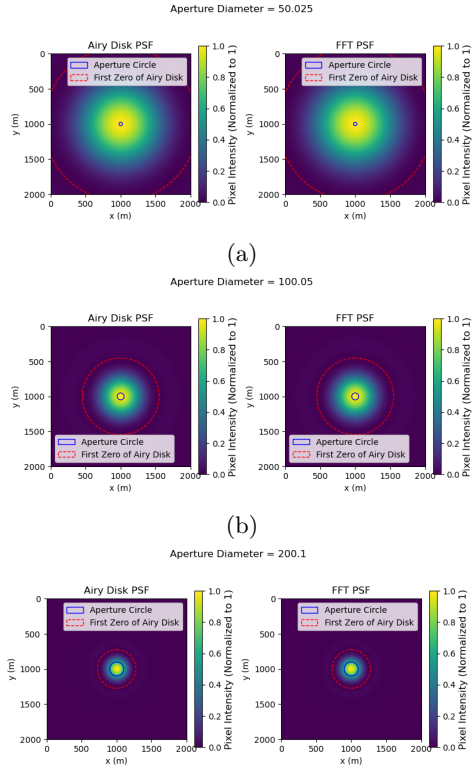

FIG. 5: Effect of Increasing Aperture Diameter on PSF calculations. The PSF calculated using the analytical Airy Disk and FFT are presented. Circles are also drawn to represent the circular aperture and the first zero of the ideal airy disk

small aperture creates a much larger image. Size of the psf focus depends inversely on the size of the aperture.

The Hubble telescope is an example of a Cassegrain reflecting telescope with primary and secondary mirrors 2.4m and 0.3m in diameter respectively and can detect objects that are 10 billion times fainter than the human eye can detect [11]. As the telescope is in orbit around the Earth it is high above the blurring effects of the atmosphere, with a resolution 10 times better that that of larger, ground-based telescopes [12]. Given that the Hubble telescope has the same structural design as the telescope in our model, the results obtained through our calculations were compared to images of stars captured by the telescope; the reason for this was to determine the relative accuracy of our computations. *Figure 6* below shows this comparison:

We've accurately shown the location of the Hubble's struts as being at 45 degrees off from the horizontal and vertical. The fft calculation on the grid also shows the ringed minima on the Hubble's diffraction spike which indicates we are doing our computations correctly. The distance between those ringed minima depends on the width of the of the struts, wider struts causing for the minima to be closer together and narrower minima mak-

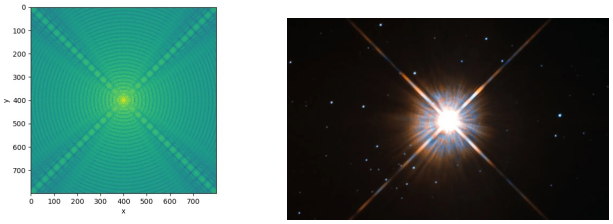

FIG. 6: Left: PSF determined using Cassegrain aperture. Right: An image taken from Hubble telescope of Proxima Centauri [13]

ing them farther apart.

III. CALCULATING PSFS IN IMPERFECT SYSTEMS

It is known that small imperfections in the mirror cause phase shifts due to the fact that they change the path length of the light in a way that depends on location in the aperture [1, 14]. Such shifts in the phase were simulated by using our aforementioned Gaussian random field function to produce a field for the phase offsets W (which has the same units as λ) in each pixel. In order to do this the power spectrum $P(k)$ was calculated for power at large k, the results of which can be seen in *Figure 7* for increasing noise levels:

These three plots were made with a the same power spectrum, but with increasing amount of noise from the base amount: 1x, 10x, and 20x, respectively. When the noise level became comparable to the actual amount of light the aperture was initially letting through the psf began to fail. Issues also began before that however. At 10x noise, while the bright center is still mostly unimpeded, the psf is getting randomly smeared and becoming unintelligible. At 20x it would be be unusable.

The point spread function can also become imperfect in ground-based telescopes due to atmospheric effects. The Earth's atmosphere causes the incoming light to not be a plane wave, instead "wrinkling" it with a coherence length of around 20cm [1]. Previous work has noted that atmospheric turbulences cause the point spread function to change elliptically [15], an effect which has also been attributed to atmospheric differential chromatic refraction (refraction effect due to the change of medium from vacuum to the Earth's atmosphere that depends on wavelength and zenith angle) [16]. Here a Gaussian random field was produced whose power spectrum cut off on small scales, and above those had fluctuations substantially larger than the wavelength of the light. The point spread function is then, in effect, acting as if the light is coming from a slightly different position in the sky. Because the plane waves of light now interfere mostly in the same way as before, but in different points in space, the point spread function becomes off center and slightly smeared

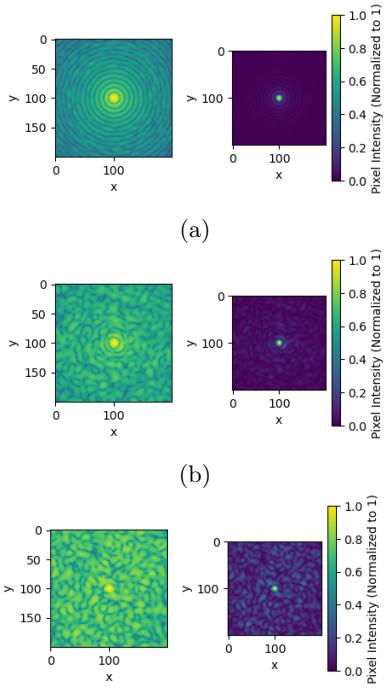

(a)

(b)

(c)

FIG. 7: Left column: log_{10} of PSF. Right column: $\sqrt{PSF}$. (a) Base level white noise applied. (b) 10 times more white noise than (a). (c) 20 times more white noise than (a).

out. The point spread function was then calculated and can be seen in *Figure 8*:

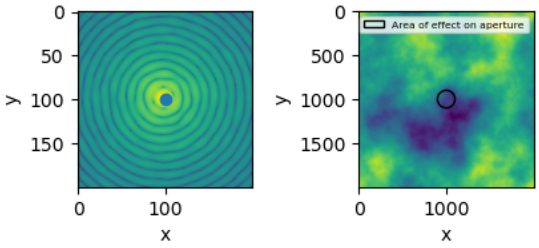

FIG. 8: Left: PSF for ground based telescope. Right: Gaussian random field used to simulate atmospheric effects.

We then wanted to simulate a long exposure by combining (in intensity) the point spread functions for many different realisations of the Gaussian random field. The individual frames of the computation were compared to the total as seen in *Figure 9*:

By averaging over many different realizations, we return back to brightest point of the point spread function being in the center and being a circle, at the cost of the outer rings becoming even more smeared out.

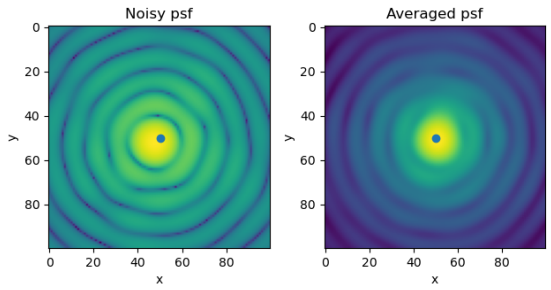

FIG. 9: Left: Single frame of noisy PSF. Right: Averaged PSF to simulate long exposure.

IV. DISCRETE VS FAST FOURIER TRANSFORM RESULT (BONUS)

(FFt requires large grid with many zeros, using a discrete fourier transform you do not have to pad a large grid with many zeros. how do these results differ?) We did not get to this part of the project.

V. CONCULSION

Point spread functions describe the response of a telescope or other light focusing system to a point source. For telescopes, which look at things very far away and more or less equivalent to a point source, this means we only need the point spread function in straight forward limits to get a good idea of how a design will act when implemented. In cases with analytic results, such as the circular aperture, this is even better because it allowed us to construct computational method for an aperture and compare it to a known result. Knowing that a method works in simpler and known cases, usually means that small modifications (in line with already present structures) will also give correct results. For us this meant that we could make predictions of how a Cassegrain telescope would be affected the addition of struts to hold the central obstruction in place. Our result, *Figure 6*, correctly predicts this with the comparison to the Hubble telescope's star image shape. An interesting computation one could do is that our own eyes have a unique pattern of seams that formed when our eyes developed. This unique pattern of seams means that every person sees stars differently! Starting with how stars look to you, you could try and figure out your seam pattern (you may have to take a train upstate to get a good look at the stars if you don't remember looking at them directly given we are in Manhattan). Given a working calculation of the point spread function, you could then add noise as we have. If you have an expectation of the type of noise that will impact your system you could then adjust your system to account for it better. Looking at Eq(1), the phase shift goes as one over the wavelength, radio waves are very long, they are less affected by atmospheric effects than visible or smaller wavelength light. Overall an interesting project in structuring code and working with others to understand a system none of us were familiar with.

[1] M. Blanton, Computational physics project / telescope diffraction limit, `https://blanton144.github.io/computational-grad/pdf/project-telescope.pdf`.

[2] T. Optics, Point spread function (psf), `https://www.telescope-optics.net/diffraction_image.htm`, accessed: 2023-12-02.

[3] R. C. M. Gai, An efficient point spread function construction method, Monthly Notices of the Royal Astronomical Society **377**, 1337 (2007).

[4] E. D. Micheli, Integral representation for bessel's functions of the first kind and neumann series, Results Math **73**, 61 (2018).

[5] Wikipedia, Cassegrain reflector, `https://en.wikipedia.org/wiki/Cassegrain_reflector`.

[6] S. Tucker, Classical cassegrain design, Starizona (2020).

[7] S. Wasmus, Comparison of point spread functions of unobscured and obscured circular apertures (2018).

[8] B. Kozintsev, *Computations With Gaussian Random Fields*, Ph.D. thesis, University of Maryland at College Park (1999).

[9] S. Conrad, The beauty of gaussian random fields, Structures Blog (2022).

[10] N. E. Database, The power spectrum, `https://ned.ipac.caltech.edu/level5/March04/Jones/Jones6_3.html`, accessed: 2023-12-04.

[11] R. V. E.J. Chaisson, The science mission of the hubble space telescope, Vistas in Astronomy **33**, 105 (1990).

[12] NASA, Hubble design, `https://science.nasa.gov/mission/hubble/observatory/design/`, accessed: 2023-12-04.

[13] T. Chao, Proxima centauri, nearest star to sun, seen by hubble telescope, (2014).

[14] D. R. J. V. L. Schifano, M. Vervaeke, Freeform wide field-of-view spaceborne imaging telescope: From design to demonstrator, Sensors (2022).

[15] M. K. L. Liaudat, J. Starck, Point spread function modelling for astronomical telescopes: a review focused on weak gravitational lensing studies, Frontiers in Space and Astronomy **10** (2023).

[16] P. B. J. Meyers, Impact of atmospheric chromatic effects on weak lensing measurements, The Astrophysical Journal **807** (2015).